Applied Physics Letters

Giant light deflection via electro-mechanical modulation of liquid crystals

Cite as: Appl. Phys. Lett. **114**, 061901 (2019); https://doi.org/10.1063/1.5083980
Submitted: 03 December 2018 . Accepted: 22 January 2019 . Published Online: 11 February 2019

Koki Imamura, Hiroyuki Yoshida, and Masanori Ozaki

Applied Physics Letters ARTICLE scitation.org/journal/apl

Giant light deflection via electro-mechanical modulation of liquid crystals

Cite as: Appl. Phys. Lett. **114**, 061901 (2019); doi: 10.1063/1.5083980
Submitted: 3 December 2018 · Accepted: 22 January 2019 ·
Published Online: 11 February 2019

Koki Imamura,[1] Hiroyuki Yoshida,[1,2,a)] and Masanori Ozaki[1]

AFFILIATIONS

[1]Division of Electrical, Electronic and Information Engineering, Osaka University, 2-1 Yamada-oka, Suita, Osaka 565-0871, Japan
[2]Precursory Research for Embryonic Science and Technology (PRESTO), Japan Science and Technology Agency (JST), 4-1-8 Honcho, Kawaguchi, Saitama 332-0012, Japan

[a)]**Author to whom correspondence should be addressed:** yoshida@eei.eng.osaka-u.ac.jp

ABSTRACT

Liquid crystals (LCs) are matter with fluidity and anisotropy and have been used in various electro-optic devices for their capability to modulate the refractive index by voltage. Here, we show that LCs are capable of electro-mechanically modulating light to cause giant light deflection at low voltages (exceeding 64° at 1.0 V). We use a composite material where polymerized cholesteric LC particles that show optical Bragg reflection float in a nematic LC medium. The polymer-particles are elastically coupled with the host director through their surface molecular anchoring and rotate from a face-on to side-on configuration at the Frederik transition. Rigid-body rotation of the reflection plane causes light deflection, which is well reproducible and can be modelled theoretically. Our findings demonstrate the capability of LCs as a micro-electrical-mechanical system platform, which are potentially useful for large-area light-controlling applications.

Liquid crystals (LCs) are matter in an intermediate phase between liquids and crystals and thus possess fluidity and anisotropy. LCs are widely used for not only flat panel displays but also other electro-optic devices since they are capable of modulating light. In these applications, nematic LCs with the simplest orientational order are commonly used because of their easy tunability of refractive indices.[1] The functionality of LCs with higher-ordered structures has also attracted intense interest for a long time due to the prospect of electro-optic modulation which cannot be realized using nematic LCs. However, because their structures are easily deformed by an electric field, reversible and continuous electro-optic modulation using them still remains a non-trivial challenge.

The cholesteric LC (ChLC) phase is one in which the constituent rod-like molecules self-organize into a helical structure and give rise to a Bragg reflection band for circularly polarized light with the same handedness as the helix.[1,2] Although ChLCs have been long known and their electro-optic response has been well-studied,[3–5] their practical use had been hindered because their structure is easily deformed by an electric field and switching becomes irreversible.[6]

Here, we propose to tune the optical properties of ChLCs by mechanically rotating the helical structure instead of deforming it. We embed disc-shaped polymer particles with a rigid cholesteric order in a nematic LC and induce its rotation by an electric field. At the Frederiks transition[7] of the host LC, the particles rotate from a face-on to side-on configuration through the elastic coupling mediated by molecular anchoring on the particle surface. The electro-mechanical rotation of the periodic structure results in continuous tuning of the reflection spectrum as well as giant light deflection with a maximum measured angle of ∼64° by a voltage as low as ∼0.9 V. In addition, no distortion occurs in the selective reflection band because a rigid cholesteric structure is physically rotated. We also show that the experimental observations are reproduced by a theoretical analysis of the system, which couples rigid-body rotation of the particle with the director deformation of the host, by constructing a combined model incorporating the free energy of the host LC and the electrostatic energy of the particle.

The photopolymerizable ChLC material was prepared by mixing a reactive mesogen mixture (Merck, RMM141C), a right-handed chiral dopant (Merck, CD-X), and a photoinitiator (TCI, 2-Benzyl-2-(dimethylamino)-4′-morpholinobutyrophenone) at a weight ratio of 93.2:4.0:2.8. The material was filled into a planar sandwich cell assembled from two glass substrates coated with a rubbed polyimide (JSR, AL1254). After confirming planar

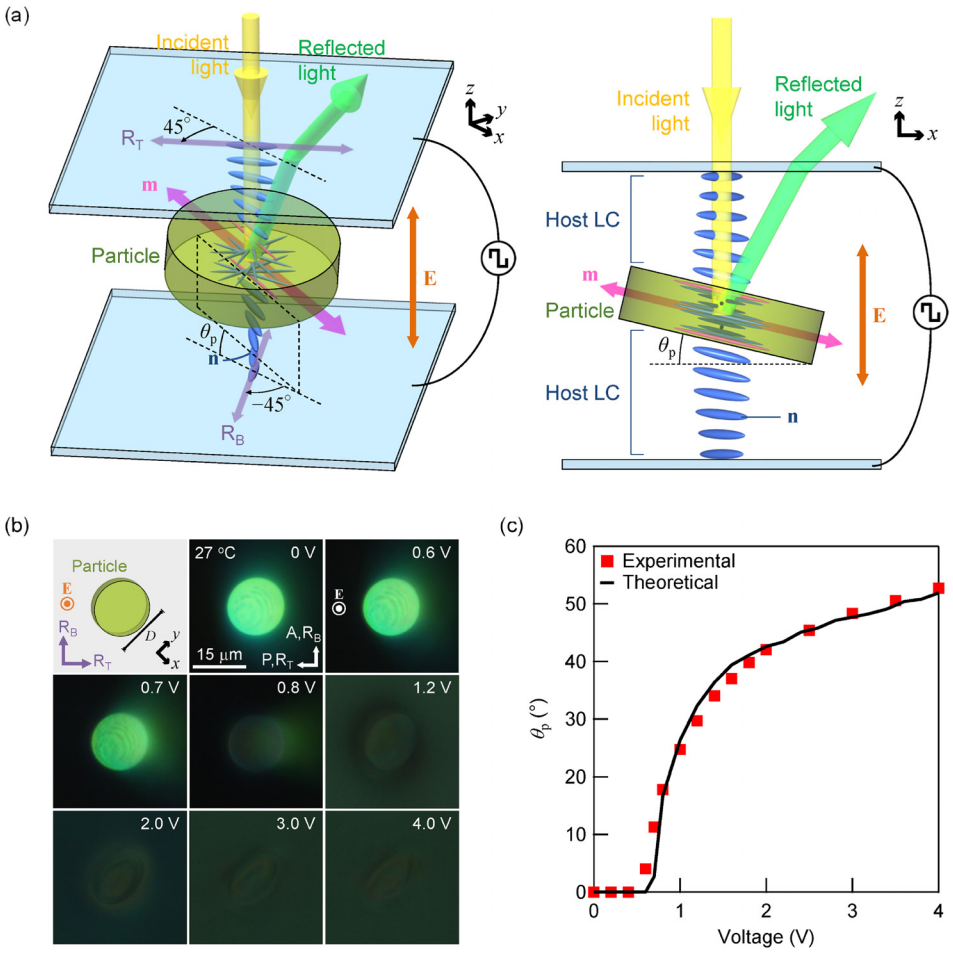

FIG. 1. (a) Schematic of the experimental configuration for observing the ChLC particle in the TN cell. The arrows labeled R_T and R_B indicate the directions of the rubbing on top and bottom substrates, respectively. (b) Schematic and POM images of the particle at different voltages. The arrows labeled P and A indicate the directions of the polarizer and the analyzer, respectively. (c) Applied voltage dependence of measured (filled squares) and theoretical (solid line) rotation angles of the particle.

orientation, the sample was placed on a commercial laser scanning microscope system (Carl Zeiss, LSM 510) to perform two-photon excited direct laser writing (DLW)[8–11] for particle fabrication. A Ti:Sapphire laser (Spectra Physics, Maitai) with a center wavelength of 800 nm, a pulse width of 100 fs, and a repetition rate of 80 MHz was tightly focused at the center of the cell by an oil-immersion objective lens (63×, NA = 1.4) and scanned over a circular area with a diameter of 15 μm at a laser intensity of 4.3 MW cm^{-2} and a scan speed of 9 μs μm^{-1}. This condition yielded disc-shaped particles with a diameter of 15 μm and a height of approximately 3 μm (measured by laser scanning microscopy). The helix axis of the ChLC in the resultant particles was along their height direction. DLW causes a pitch elongation[9,10] by approximately 20% and sets the easy axis of molecular orientation on the particle surface along the polarization direction of the laser (supplementary material note 1). Considering this pitch elongation effect, the pitch of the material was adjusted to obtain particles exhibiting a Bragg reflection band between approximately 500 and 550 nm, by adjusting the concentration of the chiral dopant. After particle fabrication, the cell was disassembled and the residual reactive mesogen was removed by an absorbent paper. The particles were then mixed with a nematic LC (Merck, 5CB) and filled in a twisted nematic (TN) cell with a cell gap of approximately 15 μm. The two substrates possessed ITO electrodes and were coated with the same polyimide used for particle fabrication, with the rubbing directions set in orthogonal directions to each other. As will be shown later, the combination of the TN structure and the unidirectional surface orientation on the particle plays an important role in achieving a reversible response to an electric field. To confirm that the unpolymerized reactive mesogens and the chiral dopant were removed, we measured the polarized transmittance spectra of the host in the TN cell and ensured that the same spectrum as that of pure 5CB was obtained (supplementary material note 2).

Observation was performed under a cross polarized optical microscope (POM; Nikon, Eclipse LV100-POL) using a 100× objective lens with a NA value of 0.90 in the reflection mode, as a rectangular voltage of frequency 10 kHz was applied between the substrates [Fig. 1(a)]. The sample temperature was controlled to 27 °C by a commercial hotstage (Linkam, LTS420). Figure 1(b) shows the POM images of the ChLC particle at various voltages.

The particle, which is at rest with its surface parallel to the substrates of the cell, rotates to become oriented side-on with increasing voltage. The rotational behavior is well reproducible, and the particle switches back to the initial state upon removal of voltage. To analyze the rotational behavior of the particle, we define the coordinate axes of the system as shown in Fig. 1(a), where the rubbing directions on the top and bottom substrates are at +45° and −45° to the x-axis, respectively. To describe the particle orientation, we define the molecular orientation on the top and bottom surface of the particle by a unit vector, **m**. At 0 V, the particle floats in the cell and aligns **m** along x, parallel to the substrates. Hereafter, we define this configuration as the initial state, i.e., $\theta_p = 0°$, where θ_p is the polar angle of **m**, measured from the x-axis. When a voltage is applied along z, the particle rotates around the y-axis, causing θ_p to increase. Figure 1(c) shows the voltage dependence of θ_p, where θ_p was evaluated by measuring the apparent shortest edge diameter of the elliptical projection of the bottom surface of particles in the POM images. The switching behavior has a threshold at ∼0.6 V and increases monotonically with an increase in voltage.

The two main contributions driving particle rotation are the electrostatic torque generated to minimize the electrostatic energy of the particle, F_{elec}, and the elastic torque generated to reduce the free energy of the nematic LC, F_{LC}.[12,13] F_{elec} in the presence of field is given by $F_{elec} = -(1/8)\varepsilon_0\Delta\varepsilon_p\pi D^2 h(\mathbf{m}\cdot\mathbf{E})^2$, where ε_0 is the permittivity of free space, $\Delta\varepsilon_p$ is the effective dielectric anisotropy of the ChLC particle, D is the particle diameter, h is the particle height, and **E** is the electric field. F_{LC} is given by $F_{LC} = \int_{LC}(f_{Frank} - (1/2)\varepsilon_0\Delta\varepsilon_{LC}(\mathbf{n}\cdot\mathbf{E})^2)dV_{LC}$, where f_{Frank} is the elastic energy density of the host LC, $\Delta\varepsilon_{LC}$ is the host dielectric anisotropy, **n** is the host director distribution, and $\int_{LC} dV_{LC}$ indicates integration over the whole host LC volume around the particle.

In the present case, **n** and **m** change depending on the applied voltage to minimize the total free energy of the system, $F = F_{LC} + F_{elec}$. Based on this model, we numerically simulated the distribution of **n** and **m** which minimize F. The model assumes that a disc-shaped particle is positioned at the center of a TN cell with no translational motion. In calculating F_{LC}, we treat the ChLC particle as a thin nematic particle with zero thickness and do not consider the influence from the side surface of the particle. A quasi-three-dimensional analysis, where the director deformation is calculated in the x–z plane and summed in the y-direction, is performed for the calculation of the distribution of **n** and **m**. As the boundary condition, strong anchoring is assumed along the rubbing direction on the substrates and along **m** on the particle surface, with a pretilt angle of θ_0. In calculating F_{elec}, its whole volume is considered. Because of the short pitch of the ChLC structure, the particle behaves approximately as a uniaxial dielectric medium, with the permittivity along its helical axis being smaller than that along **m**, yielding $\Delta\varepsilon_p \approx (\varepsilon_{||} - \varepsilon_\perp)/2$, where $\varepsilon_{||}$ and $\varepsilon_\perp$ are the permittivities of the reactive mesogen parallel and perpendicular to the director, respectively.

In the considered system, $\mathbf{m} = (\cos\theta_p, 0, \sin\theta_p)$, $\mathbf{n} = [\cos\psi(x, z)\cos\theta(x, z), \sin\psi(x, z)\cos\theta(x, z), \sin\theta(x, z)]$, and $\mathbf{E} = (0, 0, E)$, where ψ and θ are the azimuthal and polar angles of the host director, respectively. The expression for F thus becomes

$$
\begin{aligned}
F = &\int_{LC}\left(f_{Frank} - \frac{1}{2}\varepsilon_0\Delta\varepsilon_{LC}E^2\sin^2\theta\right)dV_{LC} \\
&- \frac{1}{8}\varepsilon_0\Delta\varepsilon_p E^2\pi D^2 h\sin^2\theta_p, \quad \text{where} \\
f_{Frank} = &\frac{1}{2}K_{11}\left(\sin\psi\cos\theta\frac{\partial\psi}{\partial x} + \sin\theta\cos\psi\frac{\partial\theta}{\partial x} - \cos\theta\frac{\partial\theta}{\partial z}\right)^2 \\
&+ \frac{1}{2}K_{22}\left(\sin\theta\cos\theta\cos\psi\frac{\partial\psi}{\partial x} - \cos^2\theta\frac{\partial\psi}{\partial z} - \sin\psi\frac{\partial\theta}{\partial x}\right)^2 \\
&+ \frac{1}{2}K_{33}\left\{\cos^2\theta\left(\cos\psi\cos\theta\frac{\partial\psi}{\partial x} + \sin\theta\frac{\partial\psi}{\partial z}\right)^2\right. \\
&\left. + \left(\cos\psi\cos\theta\frac{\partial\theta}{\partial x} + \sin\theta\frac{\partial\theta}{\partial z}\right)^2\right\}. \qquad (1)
\end{aligned}
$$

Here, K_{11}, K_{22}, and K_{33} are the splay, twist, and bend Frank elastic constants of the host LC, respectively, and E is the electric field strength (= V/d, where d is the cell gap and V is the applied voltage). For practical purposes of calculation, the integration ($\int_{LC} dV_{LC}$) is taken over the full thickness of the cell and the full diameter of the particle in the y-direction and extended in the x-direction from the particle edge by 10 μm. F is minimized by the finite difference method on a lattice with dimensions 500 × 1000 × 500. Using $\theta_0 = 1.8°$,[13] $K_{11} = 5.7$ pN, $K_{22} = 3.7$ pN, $K_{33} = 7.5$ pN,[14] $\Delta\varepsilon_{LC} = 12$,[15] and $\Delta\varepsilon_p = 2.5$ (= $\Delta\varepsilon_{p,N}/2$, where $\Delta\varepsilon_{p,N}$ is the dielectric anisotropy of nematic particles),[12] the simulation result shown by the solid line in Fig. 1(c) is obtained, which is in excellent agreement with the experimental results. The values used were the same as those used in the previous study, which described the motion of RMM-141C-based nematic particles conducted under the same conditions.[12]

It should be noted that coupling between the particle and the host LC, mediated by the surface anchoring on the particle, is key for achieving the well-controlled electro-mechanical response. Anchoring of LC orientation on the particle surface along **m**, which is different from the case of isotropic colloids,[16,17] induces a splay-bend deformation of the host upon particle rotation, coupling the response of the host and the particle. The TN cell structure is equally important in achieving a reproducible response since the intrinsic twist deformation of the TN cell causes the director to be deformed even for a small rotation of the particle, leading to a unique orientation configuration at rest. The reversible response originates from the system relaxing to the global ground state upon removal of the field. This is not achieved in a planar cell with parallel orientation on both substrates because the particle can rotate freely around the host director axis (**n**) without deforming the alignment (supplementary material note 3).

The mechanical rotation of the particle results in continuous changes in the intensity and propagation direction of light. The reflectance and transmittance spectra of the sample were measured for incident light polarized parallel to the rubbing direction of the cell, using a fiber-coupled multichannel spectrometer (Hamamatsu Photonics, PMA-11). The measurement spot diameter was ∼10 μm. Figures 2(a) and 2(b) show the voltage dependence of the reflectance and transmittance spectra of the particle. As a voltage is applied, the particle rotates by angle θ_p

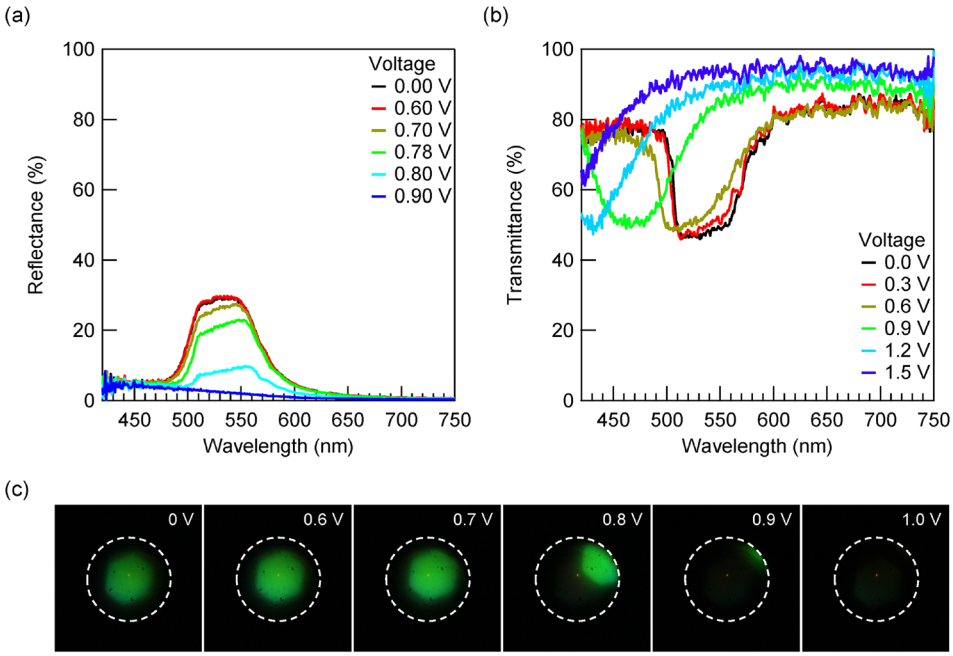

FIG. 2. Voltage dependence of the (a) reflectance and (b) transmittance spectra of the particle. (c) Voltage-dependent POM images with a Bertrand lens inserted in the optical path. Dotted circles indicate the detection limit of the deflected light (~64° in air) limited by the objective NA.

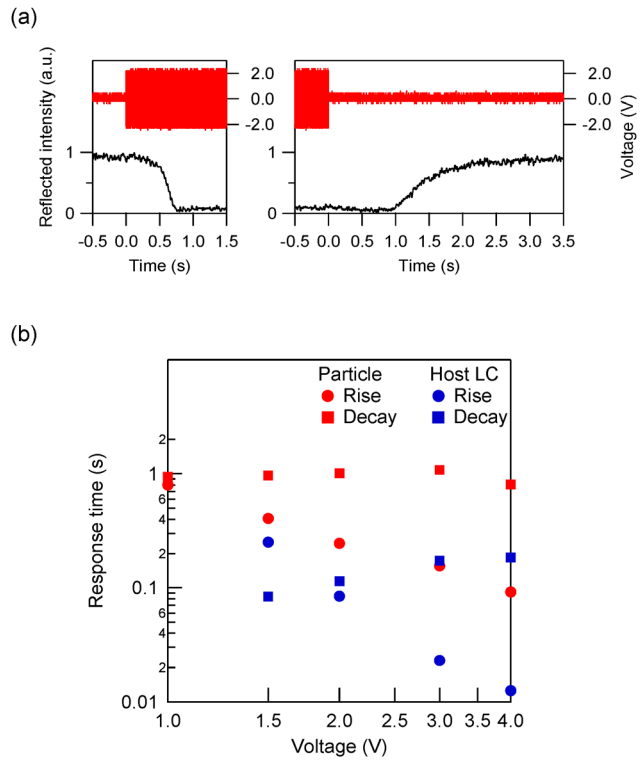

FIG. 3. (a) Transient response curves of the particle upon application (left) and removal (right) of voltage (2 V) in the TN cell. (b) Applied voltage dependence of the response time of the particle and the host LC in the TN cell.

and deflects light at an angle $2\theta_p$. The reflectance drops when the deflected angle exceeds the detection limit of the objective NA (which corresponds to $\theta_p = \sim 17°$, obtained from Snell's law assuming the average refractive index of the host LC to be 1.59[18]), and this occurs at ~0.8 V, which is consistent with the curve of Fig. 1(c). For the transmittance, a blue-shift of the reflection band is observed, caused by the increase in the effective incident angle.[19] Figure 2(c) shows the voltage-dependent POM images of the back-focal plane of the microscope objective. The green hexagon corresponds to the beam divergence angle of the incident light (~16° in air), and the white dotted circle indicates the detection limit of deflected light (~64° in air) determined by the objective NA. The distance of each hexagon from the center of the dotted line corresponds to the deflection angle of reflected light. The images clearly show light being deflected by particle rotation, with a threshold at ~0.6 V and exceeding the detection limit of 64° at ~0.9 V. This is the largest value of light deflection that has been achieved below 1 V, with no precedent in LCs or micro-electrical-mechanical systems (MEMS).[20–22]

The response characteristics were determined as a change in reflected light intensity of green light (filtered from the POM light source using a band-pass filter with a center wavelength of 532 nm and a FWHM value of 10 nm) using a photomultiplier tube (Hamamatsu Photonics, H10722). The measurement spot diameter was ~2 μm. Figure 3(a) shows typical response curves of the ChLC particle for an applied voltage of 2.0 V. Figure 3(b) shows the voltage dependence of the response time of the particle, defined as the times required for the light intensity to change from 10% to 90%, and the response times of the host, measured as the change in transmitted light intensity between crossed polarizers. The voltage dependence is similar to that of

the host, with the on-response improving with applied voltage and the off-response showing little dependence. The particle has a slower response than the host, but theoretical considerations show that the switching speeds are inversely proportional to D (supplementary material note 4), and therefore, improvement is possible by using smaller particles. Additionally, we present the response curves of the particle in a planar cell, which is much slower than the TN cell because of the absence of a global ground state (supplementary material note 5).

In conclusion, our work demonstrates the potential of LCs as an MEMS platform, where not only light intensity is modulated but also its propagation direction. Because the device has a TN structure, the concept can be extended to matrix addressing schemes, opening doors to extremely large-area light-control applications. While the response time is slower than conventional silicon MEMS, we note that it may not be a compromise in certain applications such as sunlight steering for daylighting and/or solar power concentration. While we have employed DLW for its ease in controlling the particle shape and fabrication parameters,[11–13] one can combine ChLC particles prepared by different fabrication methods, such as freeze-fracturing of polymerized ChLC films,[23,24] soft lithography,[25,26] suspension polymerization,[27] and microfluidics.[28,29] Particles with different Bragg reflection bands can be fabricated by changing the helical pitch of the polymerizable ChLC, and the reflection band can be broadened by mixing them. Mixing particles with left- and light-handed helices will lead to enhanced reflection, and holographic optical particles with programmable functionality depending on the helix phase distribution can be fabricated by patterning the ChLC alignment.[30,31] We envision ordinary LC displays being turned into dynamic mirrors, possessing the capability to control light.

See supplementary material for the basic properties of the ChLC particles fabricated by DLW (supplementary material note 1), the experimental check of the removal of the unpolymerized reactive mesogens and the chiral dopant in the host LC (supplementary material note 2), the discussion on the importance of using a TN cell instead of a parallel planar cell (supplementary material note 3), the theoretical considerations on improvement of the response times of particles (supplementary material note 4), and the response curves of the particle in a planar cell (supplementary material note 5).

This study was supported by a Grant-in-Aid for JSPS Fellows (18J10027), JSPS KAKENHI (17H02766), and JST PRESTO (JPMJPR151D). The authors thank Merck Performance Materials for providing the chiral dopant.

REFERENCES

[1]P. Yeh and C. Gu, *Optics of Liquid Crystal Displays* (Wiley, 2010).
[2]H. de Vries, Acta Crystallogr. **4**, 219 (1951).
[3]W. Hass, J. Adams, and G. Dir, Chem. Phys. Lett. **14**, 95 (1972).
[4]L. V. Natarajan, J. M. Wofford, V. P. Tondiglia, R. L. Sutherland, H. Koerner, R. A. Vaia, and T. J. Bunning, J. Appl. Phys. **103**, 093107 (2008).
[5]S. S. Choi, S. M. Morris, W. T. S. Huck, and H. J. Coles, Adv. Mater. **21**, 3915 (2009).
[6]D.-K. Yang and S.-T. Wu, *Fundamentals of Liquid Crystal Devices* (Wiley, 2006).
[7]P. G. de Gennes and J. Prost, *The Physics of Liquid Crystals* (Oxford, 1995).
[8]S. Kawata, H. Sun, T. Tanaka, and K. Takada, Nature **412**, 697 (2001).
[9]H. Yoshida, C. H. Lee, Y. Matsuhisa, A. Fujii, and M. Ozaki, Adv. Mater. **19**, 1187 (2007).
[10]H. Yoshida, Y. Miura, K. Tokuoka, S. Suzuki, A. Fujii, and M. Ozaki, Opt. Express **16**, 19034 (2008).
[11]H. Yoshida, G. Nakazawa, K. Tagashira, and M. Ozaki, Soft Matter **8**, 11323 (2012).
[12]K. Imamura, H. Yoshida, and M. Ozaki, Soft Matter **12**, 750 (2016).
[13]K. Imamura, H. Yoshida, and M. Ozaki, Soft Matter **13**, 4433 (2017).
[14]D. A. Dunmur, in *Physical Properties of Liquid Crystals: Nematics*, edited by D. A. Dunmur, A. Fukuda, and G. R. Luckhurst (INSPEC/IEE, London, UK, 2001), Chap. 5.2.
[15]R. Manohar, K. K. Pandey, A. K. Srivastava, A. K. Misra, and S. P. Yadav, J. Phys. Chem. Solids **71**, 1311 (2010).
[16]A. Choudhary and G. Li, Opt. Express **22**, 24348 (2014).
[17]S. B. Chernyshuk and O. M. Tovkach, Liq. Cryst. **43**, 2410 (2016).
[18]J. Li, S. Gauza, and S.-T. Wu, J. Appl. Phys. **96**, 19 (2004).
[19]H. Takezoe, Y. Ouchi, M. Hara, A. Fukuda, and E. Kuze, Jpn. J. Appl. Phys. Part 1 **22**, 1080 (1983).
[20]T. Roy, S. Zhang, I. W. Jung, M. Troccoli, F. Capasso, and D. Lopez, APL Photonics **3**, 021302 (2018).
[21]L. Wu and H. Xie, Sens. Actuators, A: Phys. **145**, 371 (2008).
[22]L. Ye, G. Zhang, and Z. You, Sensors **17**, 521 (2017).
[23]T. Z. Kosc, K. L. Marshall, S. D. Jacobs, J. C. Lambropoulos, and S. M. Faris, Appl. Opt. **41**, 5362 (2002).
[24]E. M. Korenic, S. D. Jacobs, and S. M. Faris, Mol. Cryst. Liq. Cryst. **317**, 197 (1998).
[25]A. Trajkovska-Petkoska, R. Varshneya, T. Z. Kosc, K. L. Marshall, and S. D. Jacobs, Adv. Funct. Mater. **15**, 217 (2005).
[26]A. Trajkovska-Petkoska, T. Z. Kosc, K. L. Marshall, K. Hasman, and S. D. Jacobs, J. Appl. Phys. **103**, 094907 (2008).
[27]E. Beltran-Gracia and O. L. Parri, J. Mater. Chem. C **3**, 11335 (2015).
[28]K. G. Noh and S. Y. Park, Mater. Horiz. **4**, 633 (2017).
[29]H. J. Seo, S. S. Lee, J. Noh, J.-W. Ka, J. C. Won, C. Park, S.-H. Kim, and Y. H. Kim, J. Mater. Chem. C **5**, 7567 (2017).
[30]J. Kobashi, H. Yoshida, and M. Ozaki, Nat. Photonics **10**, 389 (2016).
[31]M. Rafayelyan, G. Tkachenko, and E. Brasselet, Phys. Rev. Lett. **116**, 253902 (2016).